ALGORITHM FOR ESTIMATING SWIRL ANGLES IN MULTI-INTAKE HYDRAULIC INTAKES

Peetak Mitra*[1], Niranjan Gudibande [2], Kannan Iyer [2] and TI Eldho [3]

[1] -Department of Mechanical and Aerospace Engineering, Syracuse University, Syracuse, NY, USA

[2]- Department of Mechanical Engineering, Indian Institute of Technology Bombay, Mumbai, India

[3]- Department of Civil Engineering, Indian Institute of Technology Bombay, Mumbai, India

Abstract

Hydraulic Pump sumps are designed to provide a swirl free flow to the pump. The degree of swirl is measured in physical model tests using a swirl meter and a quantity known as swirl angle is generally measured. The present paper presents a novel method to compute the bulk swirl angle using the local velocity field obtained from computational fluid dynamics data. The basis for the present method is the conservation of angular momentum conservation. By carrying out both numerical and experimental studies the novel swirl angle calculation method is validated. Further the effect of vortex suppression devices in reducing the swirl angle is also demonstrated.

Introduction

Hydraulic pump sumps commonly used in circulating water cooling systems for power generation plants are required to be designed appropriately as it greatly influences the performance of the pumps and their efficiency. A non-uniform approach flow can cause the fluid in the pump intake pipe to swirl. This swirling flow if ingested by the pump can cause noise and vibration, thereby increasing the operational and maintenance costs [1]. A typical multi-intake pump sump consists of multiple inlet channels, a transition region, forebay and pump bay areas. Standards have been evolved for the design of the pump intake by Hydraulic Institute [2] for its satisfactory performance. Hydraulic Institute [2] has also suggested a procedure to perform scaled model tests and assess the quality of flow in the intake pipe using a swirl meter and recommends the measured swirl angles to be limited to less than a prescribed limit. Often due to

some constraints in the construction site, certain compromises have to be made that may require some deviations from the suggested dimensions for the pump intake. In such cases, scaled physical model tests are carried put to ensure the adequacy of the design.

The pump sump has been studied experimentally using scaled model laboratory tests [3-7]. Such laboratory tests have helped in understanding the vortex formation process, but they are expensive and take time to construct and operate. Further, detailed velocity fields, which would help the engineers to evolve better design of pump sumps, cannot be obtained in experiments.

The advancement in high speed computing and development of robust turbulence modelling techniques as well as evolution of accurate numerical algorithms in the last few years have led to the development of Computational Fluid Dynamics (CFD) codes. These have provided an alternative means to study the hydraulic flow characteristics of pump sumps. There have been several studies [8-12] in the application of CFD to model flows in pump sumps. These studies have been conducted for idealized single intake rectangular geometry. Practical pump sumps however have multiple-intakes and the disturbances in the forebay diffusion area may be carried to the pump thereby altering the flow patterns and inducement of swirls at the pump inlet. While the studies [8-12] have identified the regions of vortex formation and compared them with experiments and described swirl qualitatively (with streamlines), quantification of the swirl in terms of swirl angles that enables comparison of the numerical results with the field data has not been made.

Chen and Guo [14] have conducted simulations in the pump sump where the forebay diffusion area was also modeled. The results were benchmarked by comparing the velocity profiles at various locations with the experimental results. The flow was qualitatively analyzed by studying the streamlines and vector plots at various locations in the pump sump. However quantitative results in terms of swirl angles at the pump inlet were not presented. Desmukh et al [15] have conducted simulations on multi-intake hydraulic structures and qualitatively analyzed the flow structure. However rigorous benchmarking of the simulation with experiments was not carried out.

From the current literature, it is observed that there is a gap between the way pump sumps are qualified by physical model tests and computation methods. While the former gives a simple elegant quantitative measure for swirl in the intake the later appear to use qualitative measures. It

is also surprising that such a void exits considering that these techniques have been coexisting for over two decades.

The objective of the present work is to close this gap by evolving a method to quantify the swirl angle as used by Hydraulic Institute from the velocity field obtained from CFD. The CFD analysis is carried out in the commercial code Fluent. This has been made from first principles by using conservation of angular momentum. This method has been qualified using field tests carried out at Indian Institute of Technology, Bombay. The paper also provides some of the guidelines on the corrective actions that can be implemented to minimize the swirl angles.

CFD Methodology

The flow and the pressure fields in the pump sump are analyzed by numerically solving the full three-dimensional Reynolds Averaged Navier Stokes equation (RANS) using the commercial code Fluent.

Governing equations

The governing equations namely the continuity and Reynolds averaged momentum equations are

$$\frac{\partial}{\partial x}(u) + \frac{\partial}{\partial y}(v) + \frac{\partial}{\partial x}(w) = 0 \quad (1)$$

The momentum equations are

$$\frac{\partial}{\partial x}(\rho uu) + \frac{\partial}{\partial y}(\rho vu) + \frac{\partial}{\partial x}(\rho wu) = \frac{\partial}{\partial x}\left(\mu_{eff}\frac{\partial u}{\partial x}\right) + \frac{\partial}{\partial y}\left(\mu_{eff}\frac{\partial u}{\partial y}\right) + \frac{\partial}{\partial z}\left(\mu_{eff}\frac{\partial u}{\partial z}\right) - \frac{\partial p}{\partial x} \quad (2)$$

$$\frac{\partial}{\partial x}(\rho uv) + \frac{\partial}{\partial y}(\rho vv) + \frac{\partial}{\partial x}(\rho wv) = \frac{\partial}{\partial x}\left(\mu_{eff}\frac{\partial v}{\partial x}\right) + \frac{\partial}{\partial y}\left(\mu_{eff}\frac{\partial v}{\partial y}\right) + \frac{\partial}{\partial z}\left(\mu_{eff}\frac{\partial v}{\partial z}\right) - \frac{\partial p}{\partial y} - \rho g \quad (3)$$

$$\frac{\partial}{\partial x}(\rho uw) + \frac{\partial}{\partial y}(\rho vw) + \frac{\partial}{\partial x}(\rho ww) = \frac{\partial}{\partial x}\left(\mu_{eff}\frac{\partial w}{\partial x}\right) + \frac{\partial}{\partial y}\left(\mu_{eff}\frac{\partial w}{\partial y}\right) + \frac{\partial}{\partial z}\left(\mu_{eff}\frac{\partial w}{\partial z}\right) - \frac{\partial p}{\partial z} \quad (4)$$

The effective viscosity μ_{eff} is computed using the two equations model (k – ε) model of Launder and Spalding [16]. The equations for the turbulence kinetic energy (k) and its dissipation rate (ε) are

$$\frac{\partial}{\partial t}(\rho k) + \frac{\partial}{\partial x_i}(\rho k u_i) = \frac{\partial}{\partial x_j}\left[\left(\mu + \frac{\mu_t}{\sigma_k}\right)\frac{\partial k}{\partial x_j}\right] + G_k - \rho\varepsilon \quad (5)$$

$$\frac{\partial}{\partial t}(\rho\varepsilon) + \frac{\partial}{\partial x_i}(\rho\varepsilon u_i) = \frac{\partial}{\partial x_j}\left[\left(\mu + \frac{\mu_t}{\sigma_k}\right)\frac{\partial k}{\partial x_j}\right] + C_1\frac{\varepsilon}{k}(G_k) - C_2\rho\frac{\varepsilon^2}{k} \quad (6)$$

Here G_k represents the generation of turbulence kinetic energy due to the mean velocity gradients. The values of the constants σ_k, $C_{1,}C_2$ are those which are reported in Launder and Spalding [16].

Swirl angle calculation

Swirl angle is an important parameter to determine the quality of the flow ingested by the pumps. Hydraulic Institute [2] prescribes the method that needs to be employed for estimating this parameter. Experimentally the swirl is measured using a swirl meter shown in figure 1. The swirl meter consists of a straight vaned propeller with four vanes as shown in figure 1(b). It is mounted on a shaft on a shaft with low friction bearings. The vane diameter and the vane length are is 0.75D and 0.6D respectively, where D is the suction pipe diameter. The swirl meter is inserted into the suction pipe of the pump at a distance of 4D from the pump bell as shown in figure 1(a). The revolutions per unit time of the swirl meter are measured, and the swirl angle is then computed as

$$\theta = \tan^{-1}\frac{\omega r}{\bar{v}} \tag{7}$$

Here ω, r are the angular velocity and the radius of the vortimeter and $\bar{v}$ is the average axial velocity in the pipe.

The physical principle used in the estimation of the bulk swirl angle in the present work is that in the absence of torque the angular momentum in a given direction will be preserved. As there will be distribution of angular momentum, the total angular momentum **P** can be computed as

$$\int_A (\mathbf{r}\times\mathbf{v})(\rho\mathbf{v}.\hat{n}dA) = \mathbf{P} \tag{8}$$

The bulk angular velocity can be obtained by the equation

$$\boldsymbol{\omega}\int_A (r^2)(\rho\mathbf{v}.\hat{n}dA) = \mathbf{P} \tag{9}$$

In order to reduce the equation 9 in terms of the velocity field provided by CFD, the following methodology is adopted. Fluent provides the Cartesian velocity distributions of u, v, w in the x, y, and z directions respectively. In the present work the coordinate system has been chosen so that *y* direction represents the axial flow direction in the pipe (refer figure 1). By equating the *y* component of the angular momentum **P** in equation 8 and 9 the bulk angular momentum in *y* direction can be obtained after some simplification as

$$\omega = \frac{\int_A (\mathbf{r} \times \mathbf{v}).\hat{j}(\rho v dA)}{\int_A (r^2)(\rho v dA)} \tag{10}$$

Having obtained the angular velocity in the axial direction from equation 9, the swirl angle can be computed using equation 7.

Model Description

The multi-intake sump model used in the present study is shown in figure 2. This model has two intakes/inlets, which feed water to the common intake channel. The intakes have been designed with sufficient length to allow the flow to become fully developed and eliminate any adverse effects on approach flow distributions. The water from the intake channel then enters the transition area. In the transition area, the depth of the channel is gradually increased to the depth of the forebay area. The depth of the forebay is designed keeping in mind the required minimum submergence value as per [2]. In the forbay diffusion area width is gradually increased, to decrase the approach velocities to the pumpbay. Hydraulic Institute [2] recommends that the maximum approach velocities be limited to 0.5m/s to prevent the formation of air core vortices. The water then enters the pump intake pipe after being trained by the curtain wall. The dimensions of pump sump are shown in figures 2a and 2b. The dimensions in figure 2 are marked in terms of the pump bell diameter. In the CFD simulations the intake pumps have been modeled with zero thickness based on the work Li et al. [16] who report negligile influence of the pump wall thickness on the computed flow characterstics.

Experimental setup

Experiments were conducted on the model and the results were obtained in terms of velocity distributions and swirl angle variation. The sump was constructed of MS and acrylic sheet for visibility and to study the flow pattern. The sides and bottom of the pump chamber was provided with clear acrylic sheet for proper flow visualization. The sides and bottom of sump chamber was modeled with MS plate. The sump chamber sides and inlet channel to sump were made out of MS sheets. The suction bell mouth was made using acrylic material. The individual pumps were designed as siphon pipes with valves to control the flow. The discharge from the siphon pipes were received in the downstream tank and returned to the upstream tank by pumps. The

model was setup on an elevated platform to get a pressure head of approximately 3m for siphoning of water to simulate the pumping.

Computational mesh

The CAD model for the flow domain was made using Solidworks software and the mesh was created using ANSYS mesh generating software. Hybrid meshes consisting of both hexahedral and tetrahedral meshes were employed. Figure 3 shows the mesh employed in the present study. A total of 1.6 million cells were used in the present work. Since the standard wall functions [16] were used, the y+ was ensured to be within the acceptable range of 30 to 300.

Boundary conditions

The inlet discharge is specified as a mass flow rate and the intake pipe outlet is modeled as a pressure outlet. The Reynolds number at each of the inlets is 400,000 to simulate actual rated pump characteristics. The inflow boundary condition is treated as uniform. The water-air free surface is modeled as a shear free impenetrable wall. While strictly one needs to include free surface effects by using the volume of fluid method, it multiplies computational complications. Hence as an engineering approximation the free surface is usually modelled as a free shear wall. All other walls are assumed to have no slip boundary condition. The boundary conditions employed are clearly illustrated in figure 4. The transported turbulence characteristics are also provided at the inlet with the turbulence intensity specified as that for a fully developed pipe flow

$$I = 0.16(Re_{DH})^{-1/8} \quad (12)$$

Where (Re_{DH}) is the Reynolds number based on the pipe hydraulic diameter, $d_{h.}$ The turbulent kinetic energy k is calculated as $k = \frac{3}{2}(\bar{u}I)^2$ and the turbulence dissipation rate, ϵ is calculated as $\varepsilon = {0.1643k^{1.5}}/{l}$, for l as the turbulence length scale calculated as $l = 0.07L$, for L as the physical size of the obstruction. The computation time for each simulation was roughly 14 hours using parallel computation with Intel Xeon Dual core processor 31230 with 64 GB of RAM.

Solution Schemes

The pressure based incompressible solver is employed in the present study. The pressure velocity coupling is carried-out using SIMPLE algorithm [17]. The iteration was carried till the scaled residues fell below 10^{-4} to ensure proper convergence. Convergence was further ensured by computing the global mass balance. The spatial discretization schemes employed for pressure, momentum, turbulent dissipation rate and turbulent kinetic energy are summarized in Table 1.

CFD Validation study

To validate the CFD methodlogy employed in the present work the numerical velocity profiles at various locations were compared with the experimental results conducted in Hydraulics lab of Indian Institute of Techlology Bombay using the setup described in section 3.1. The local velocity was measured at four different cross sections as indicated in figure 5(a). In each of the cross section the velocities were measures at nine points as shown in figure 5(b). The velocities in the experiments were obtained using P-EMS (Programmable Electro-Magnetic Systes) velocity meter. The measured velocities are shown in table 2. The axial and the transverse velocity profiles obtained in simulations are compared with the experimental results in figure 6 (a-d) and (e-h) respectively. The favorable match between the experimental and the numerical results validates the CFD modelling methadology.

Results and Discussions

The simulation and experiments were performed for three cases of operating pumps: (a) all pump working, (b) two pump working, (c) single pump working. The velocity streamlines are plotted for the case when all the pumps are working in figure 4. It can be seen form figure 7(a) that the flow enters form the two inlets channel smoothly. Due to the diverging section in the transition zone the flow separates as shown in figure 7(b). The water is further slowed down in the forebay area due the increased cross section. This creates disturbances in the pump bay area as evident by the chaotic streamlines observed in figure 7(b). Most of the chaotic motion however is killed as the flow enters the pump bay area. The streamlines near the pump intake pipe (refer figure 7(b)) indicate a swirling motion. The swirl angles were calculated numerically by the method described in section 2.2. The swirl angles at 4 diameter distance from the pump bell entrance computed from the numerical simulations and experimental results are summarized in table 3.

The close match between the computed and measured results validates the swirl angle methodology described in section 2.2

Effectiveness of vortex suppression devices in reducing swirl

The swirl angle reported in the tables 3 show that the maximum swirl angle is 4.36^{o}. This is close to the maximum swirl angle limit of 5^{o} suggested by Hydraulic Institute [2]. Vortex suppression device can be used to supress the swirling motion in the pump suction. The vortex breaker designed based on [2] is shown in figure 9 is used in the present work. Experiments and simulations were run with the vortex breaker placed coaxially in the pump centerline. The swirl angles obtained after implementation of the vortex breakers is summarised in table 4. It can be seen from table 4 that the vortex breaker has reduced the swirl angles substancially. To further undertand how the vortex breaker affects the flow patters streamlines in the intake pumps have been plotted in figures 11 for the cases without and with vortex suppression devices. It can be seen tha the swirling flow is nearly supressed with the vortex breaker.

Conclusion

A new method has been presented to calculate swirl angles from the velocity field obtained from CFD to a single value which is consistent with the HI standard method [2]. Comparisons have been made between the swirl angle calculation methodology and experimentally obtained values and it is concluded that the numerical calculation method compares well. The effectiveness of the vortex suppression devices has also been demonstrated and serves as a swirl angel check.

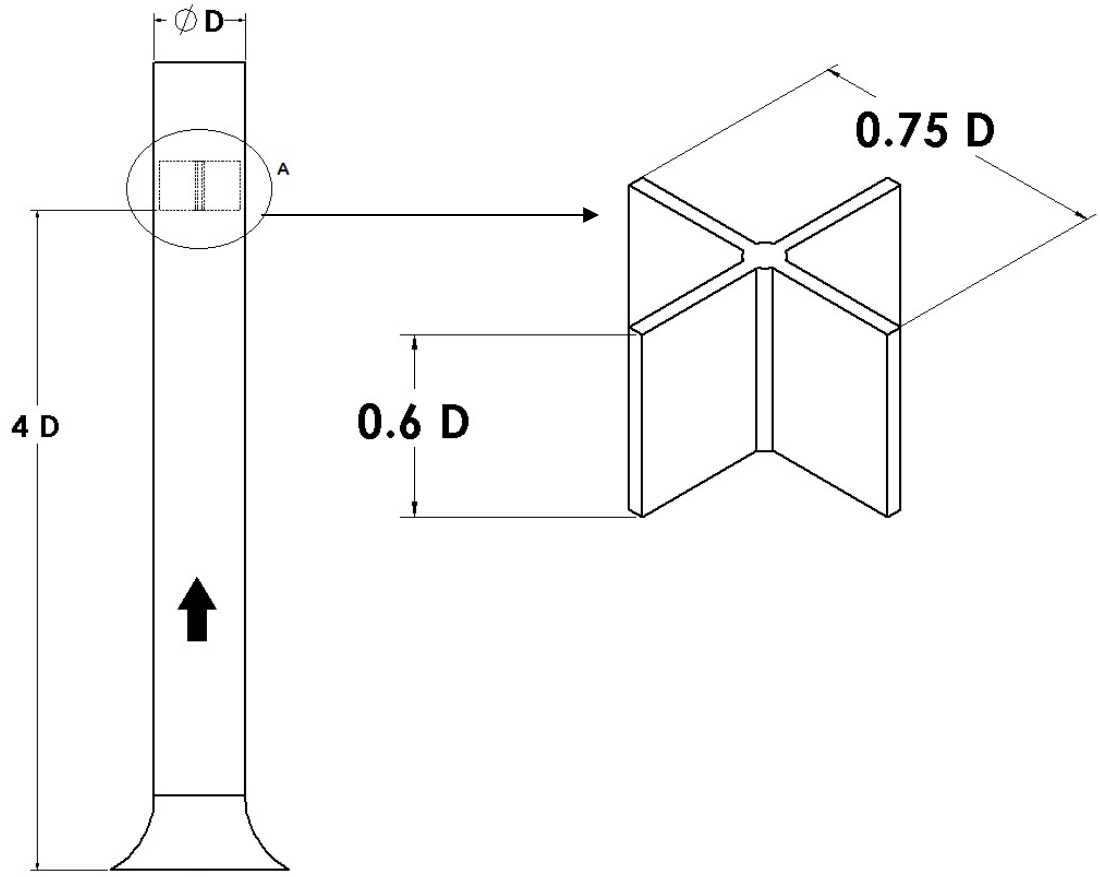

Figure 1 (a) Schematic of swirl meter (b) Details of the swirl-meter

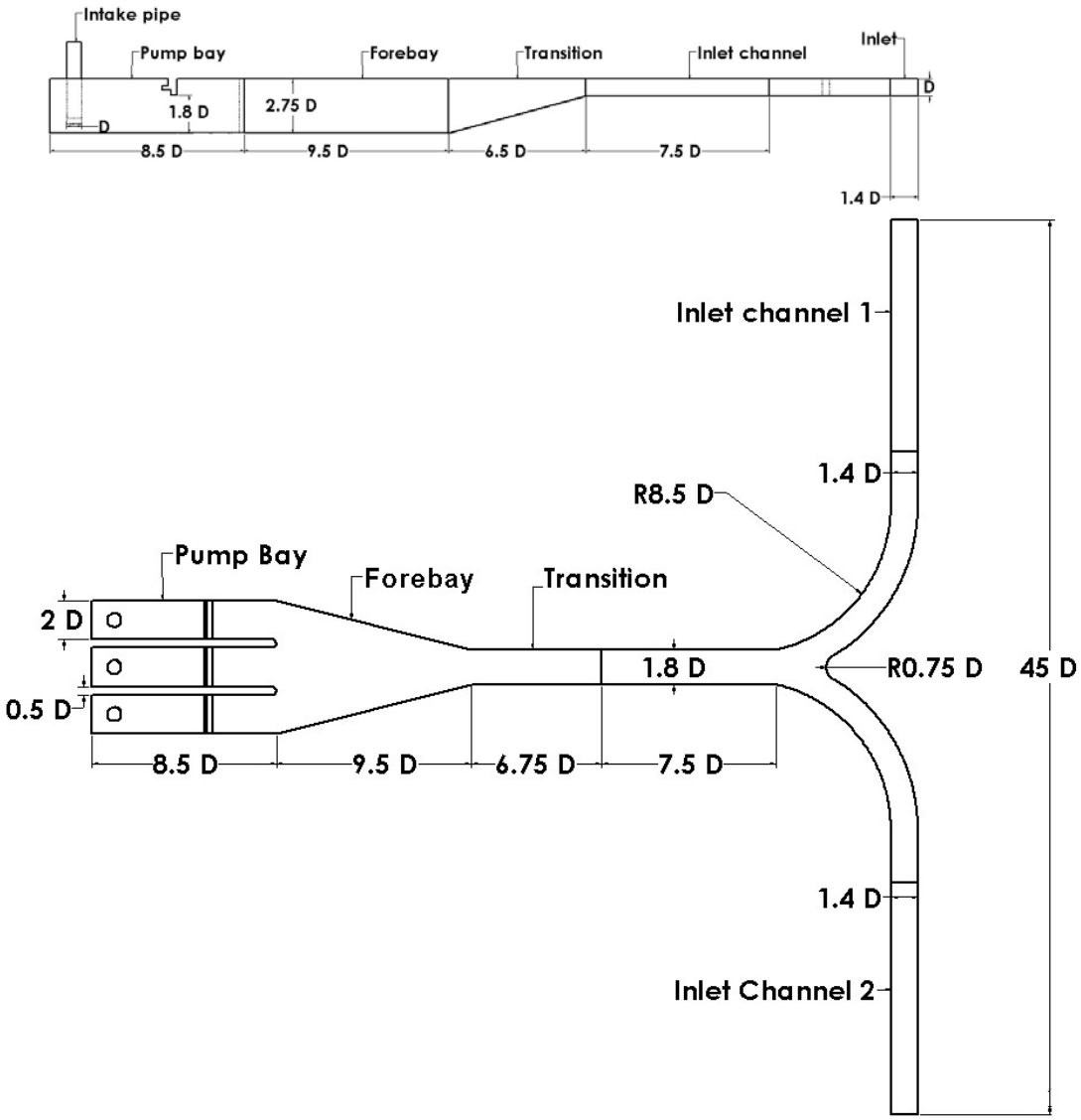

Figure 2. Model with dimensions (a). Elevated view of model (b) Top view of Model

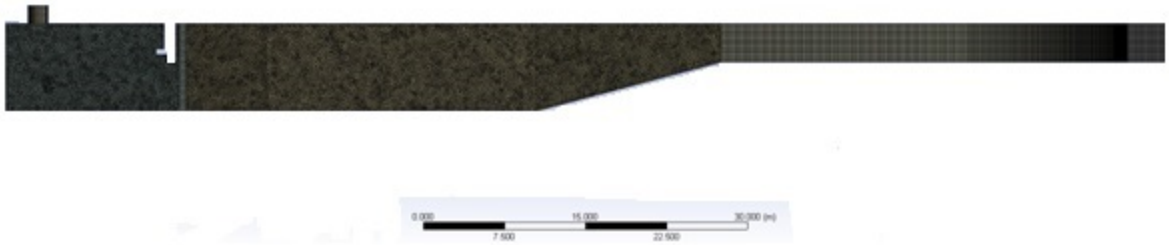

(a)

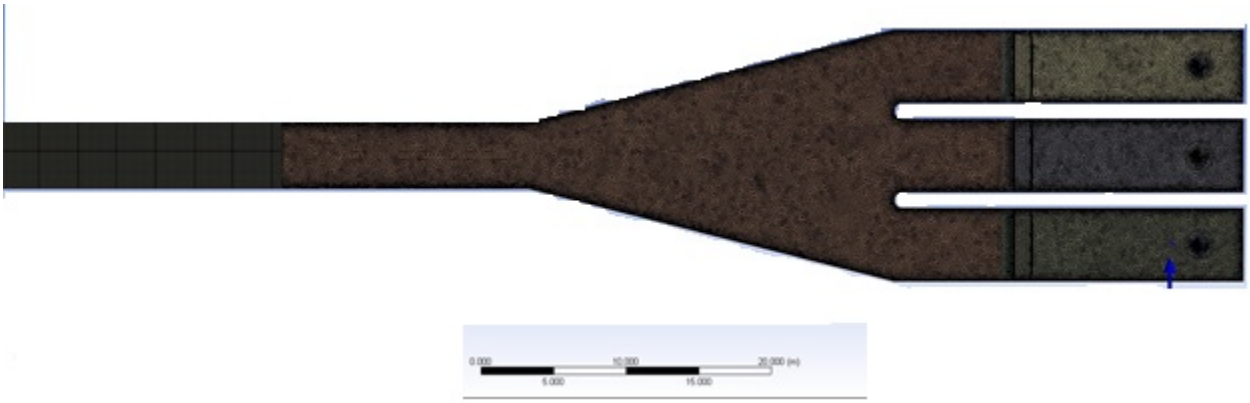

(b)

Figure 3 Mesh employed in CFD calculations (a) Side view (b) Top view showing the pump bay and transition area

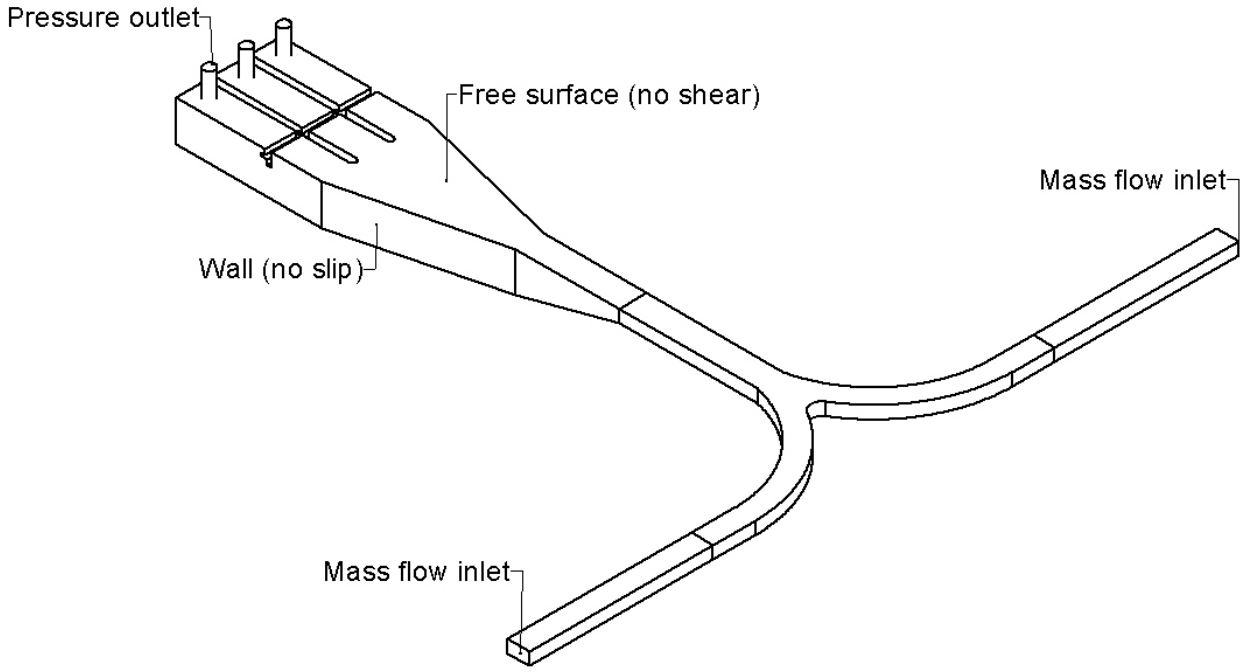

Figure 4. Boundary condition for numerical simulation

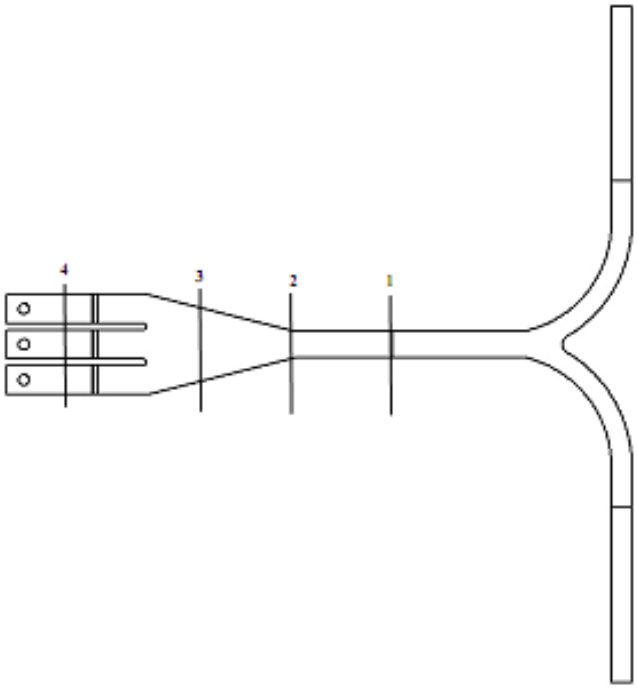

(a)

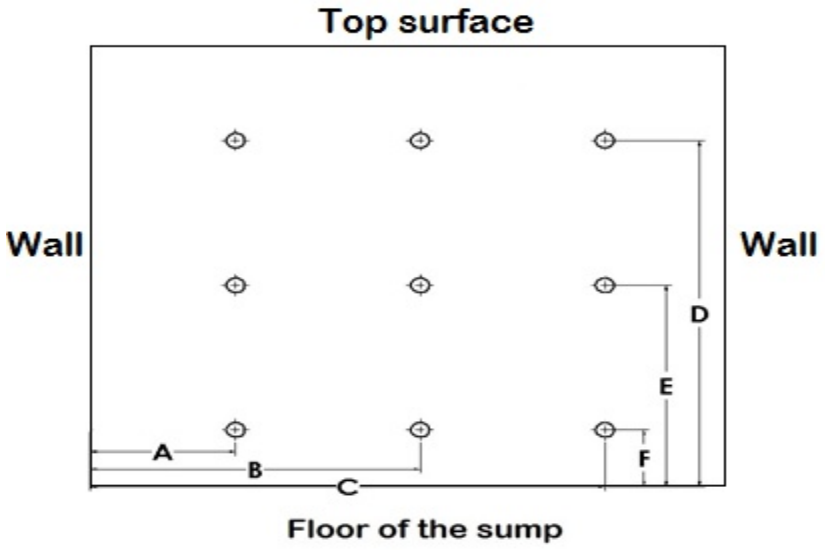

(b)

Figure 5 (a) Locations and (b) Grid points where velocities were calculated.

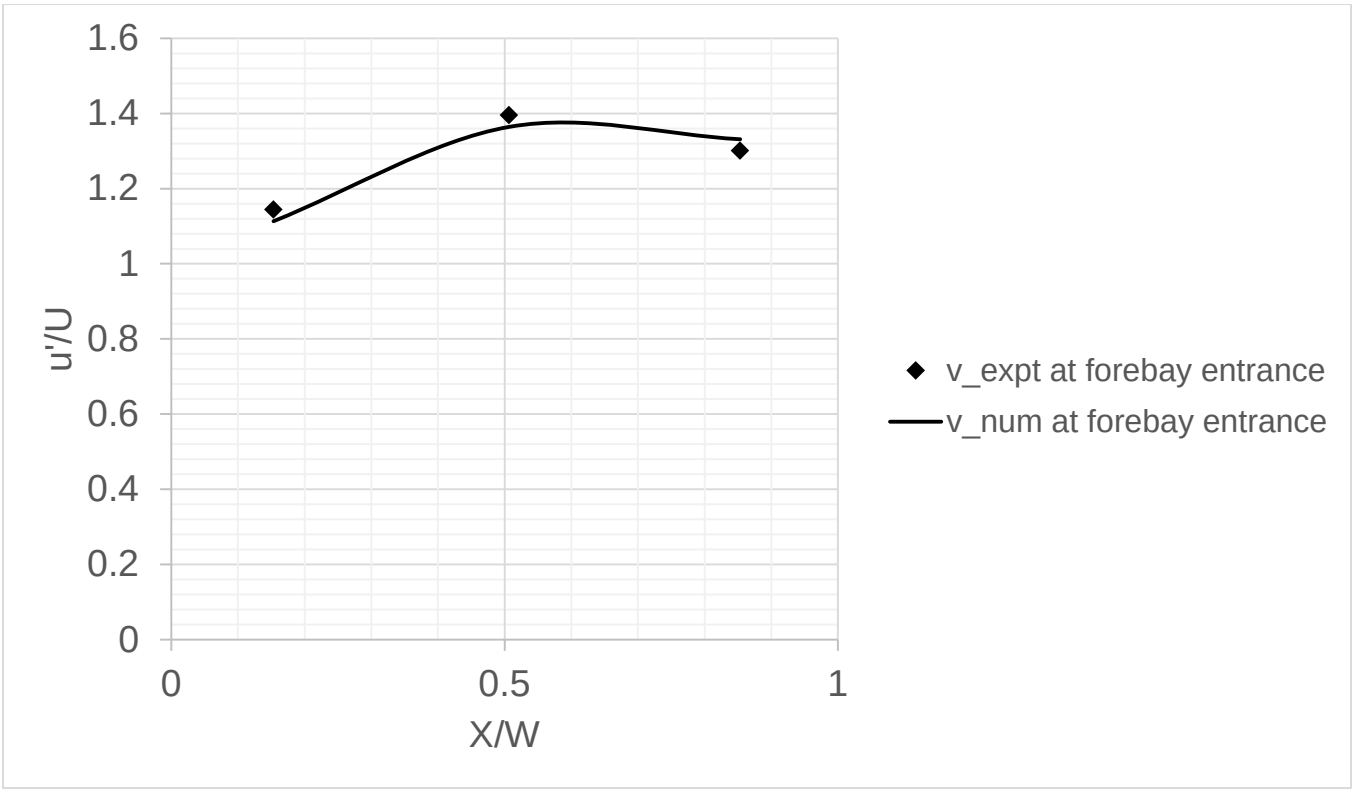
1.6
1.4
1.2
1
0.8
0.6
0.4
0.2
0
u'/U
0
0.5
1
X/W
v_expt at forebay entrance
v_num at forebay entrance

(a)

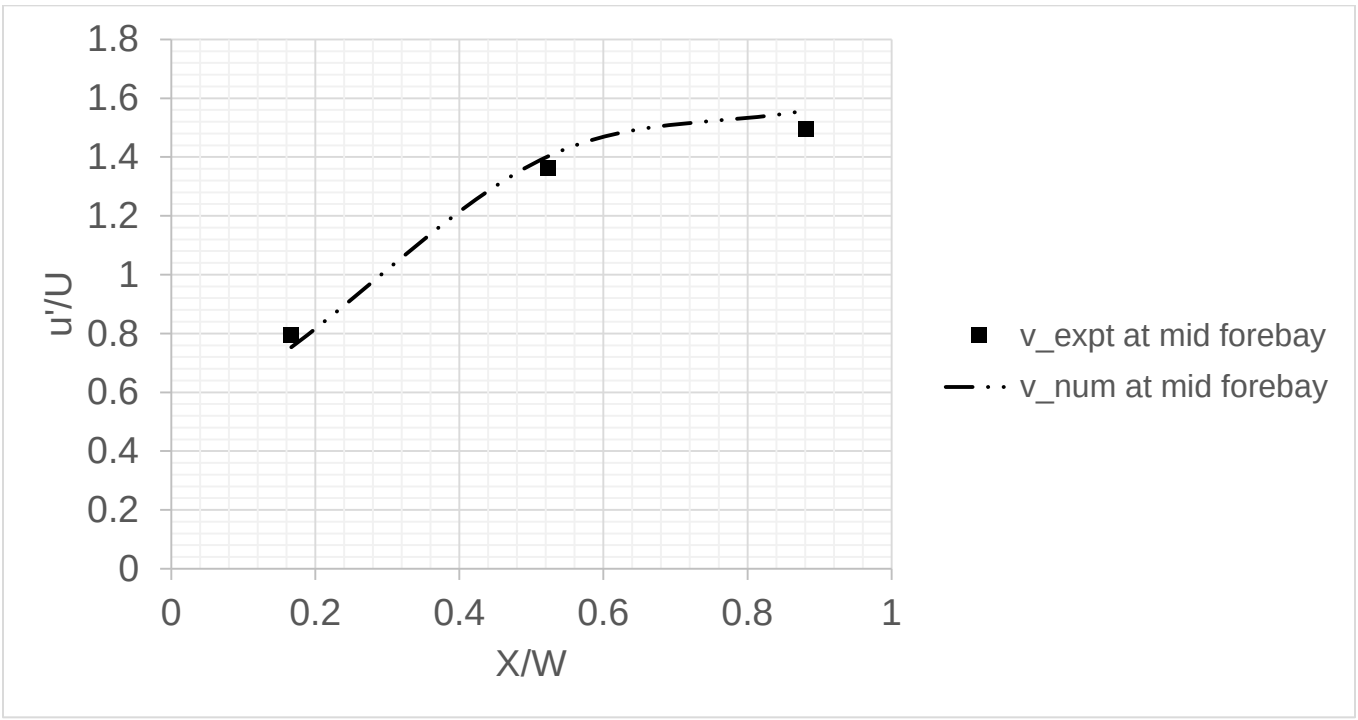
1.8
1.6
1.4
1.2
1
0.8
0.6
0.4
0.2
0
u'/U
0
0.2
0.4
0.6
0.8
1
X/W
v_expt at mid forebay
v_num at mid forebay

(b)

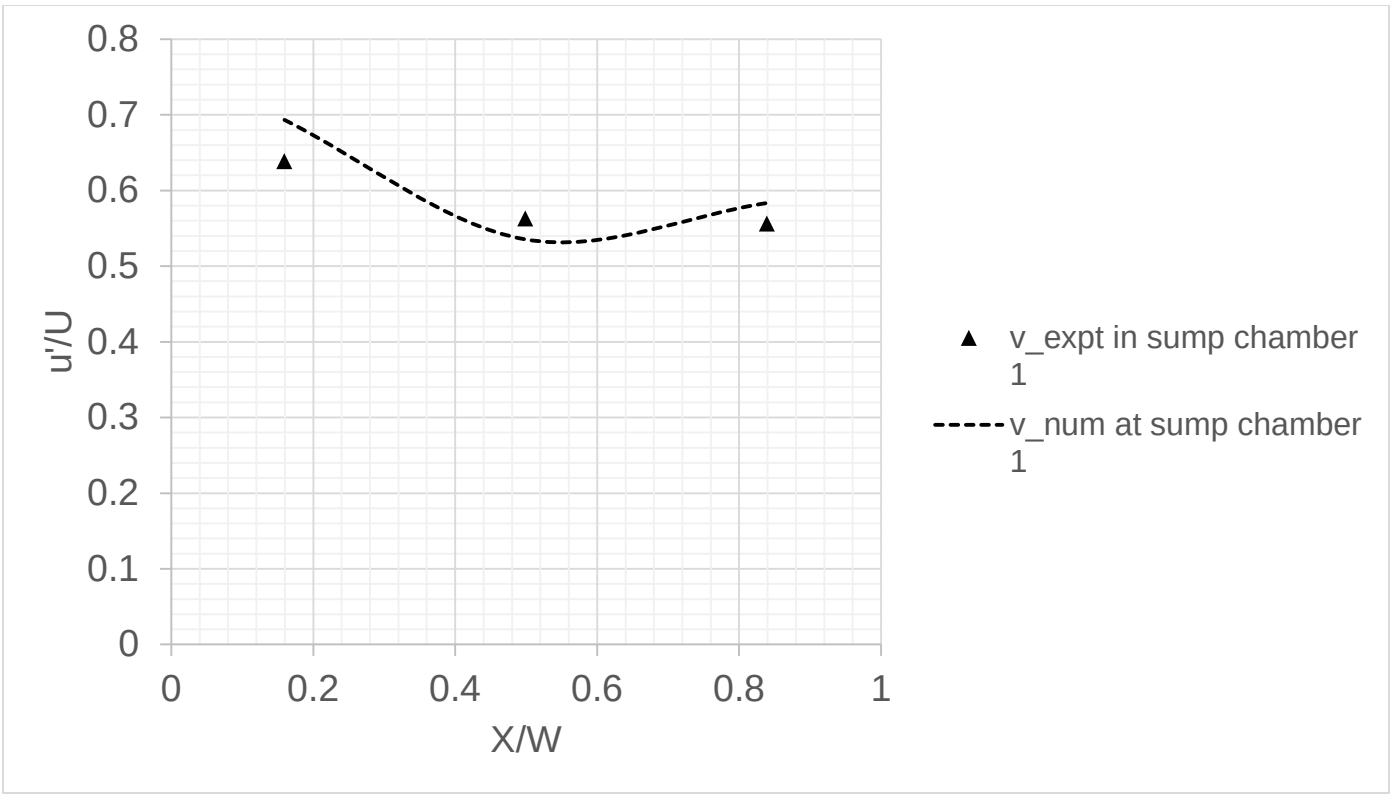
0.8
0.7
0.6
0.5
0.4
0.3
0.2
0.1
0
u'/U
0
0.2
0.4
0.6
0.8
1
X/W
v_expt in sump chamber 1
v_num at sump chamber 1

(c)

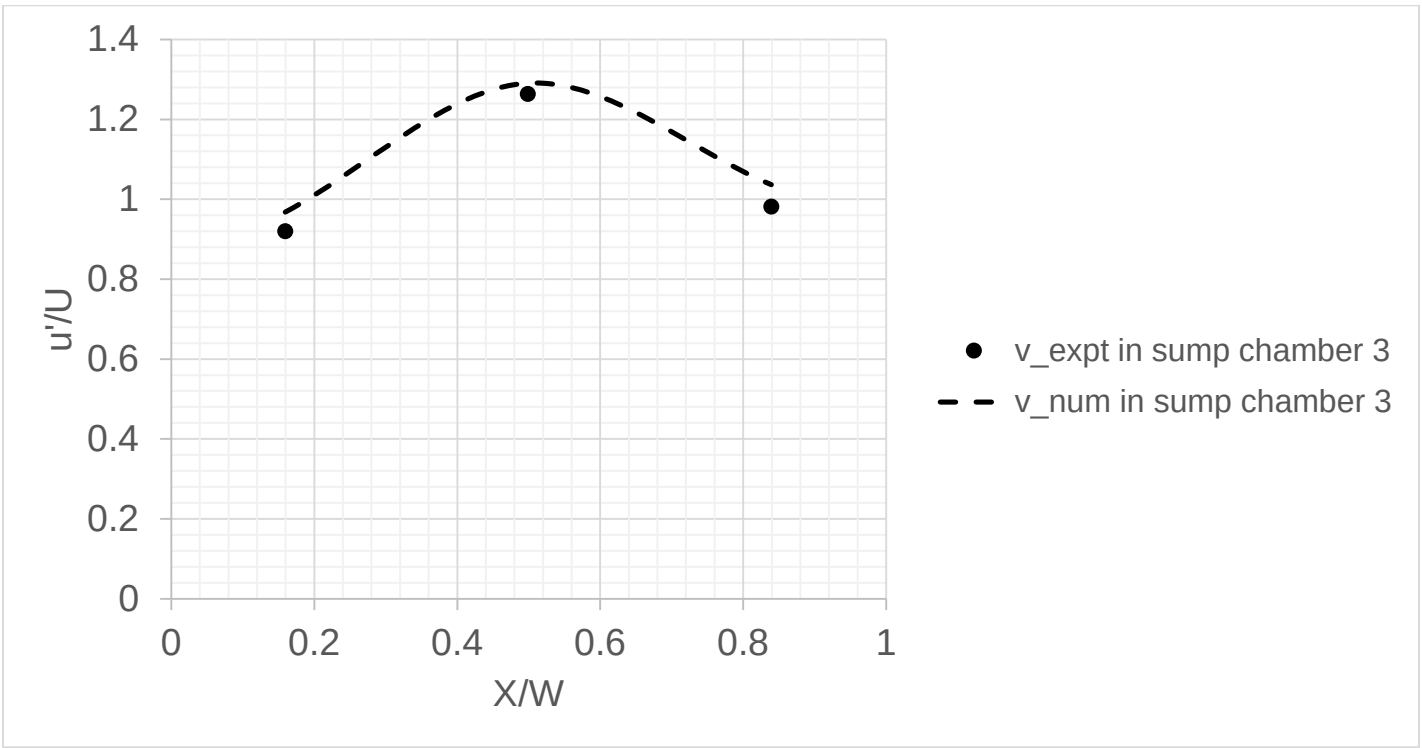
1.4
1.2
1
0.8
0.6
0.4
0.2
0
u'/U
0
0.2
0.4
0.6
0.8
1
X/W
v_expt in sump chamber 3
v_num in sump chamber 3

(d)

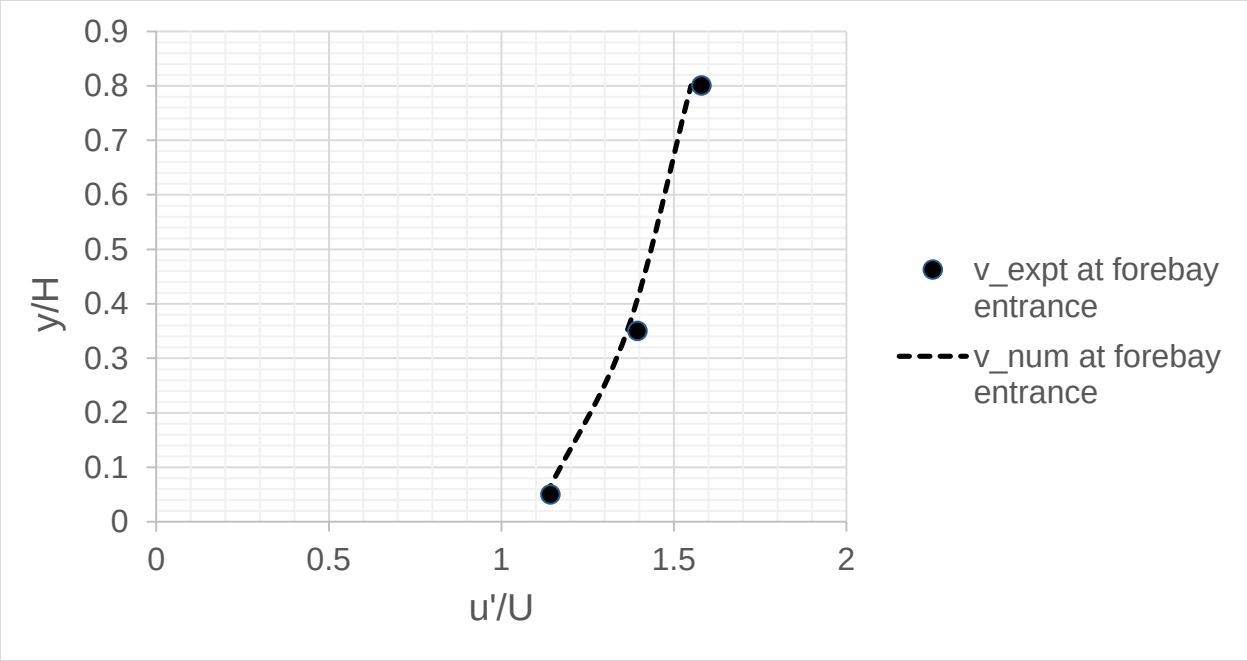
0.9
0.8
0.7
0.6
0.5
0.4
0.3
0.2
0.1
0
y/H
0
0.5
1
1.5
2
u'/U
v_expt at forebay entrance
v_num at forebay entrance

(e)

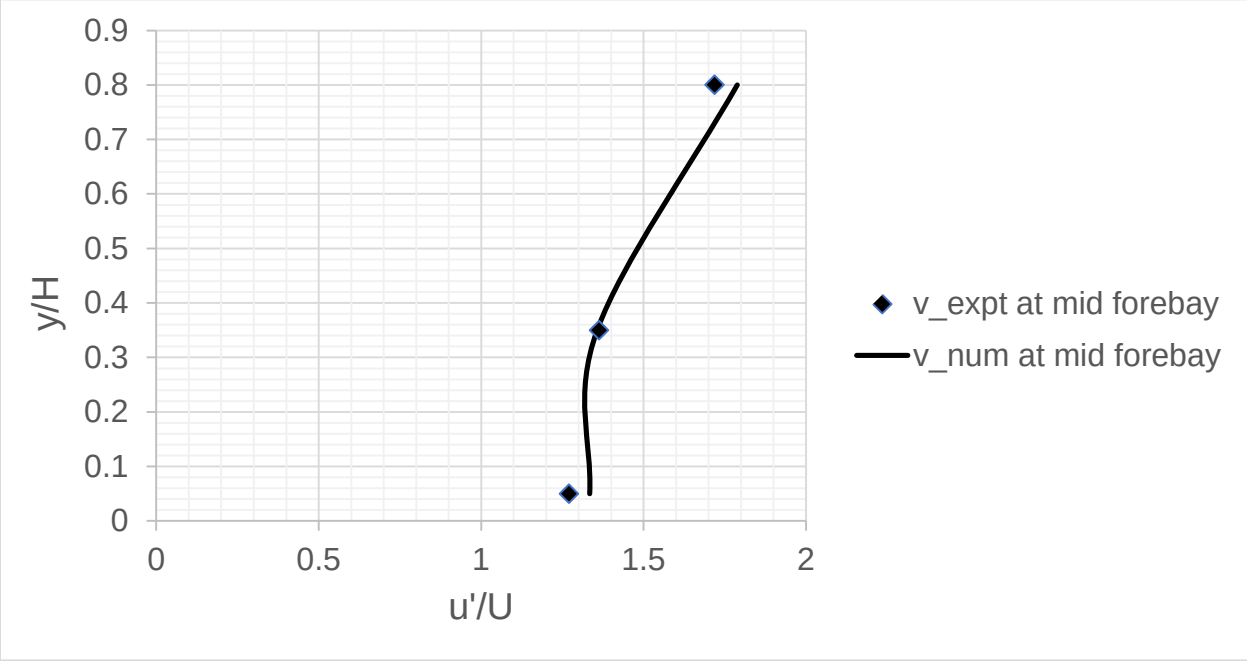
0.9
0.8
0.7
0.6
0.5
0.4
0.3
0.2
0.1
0
y/H
0
0.5
1
1.5
2
u'/U
v_expt at mid forebay
v_num at mid forebay

(f)

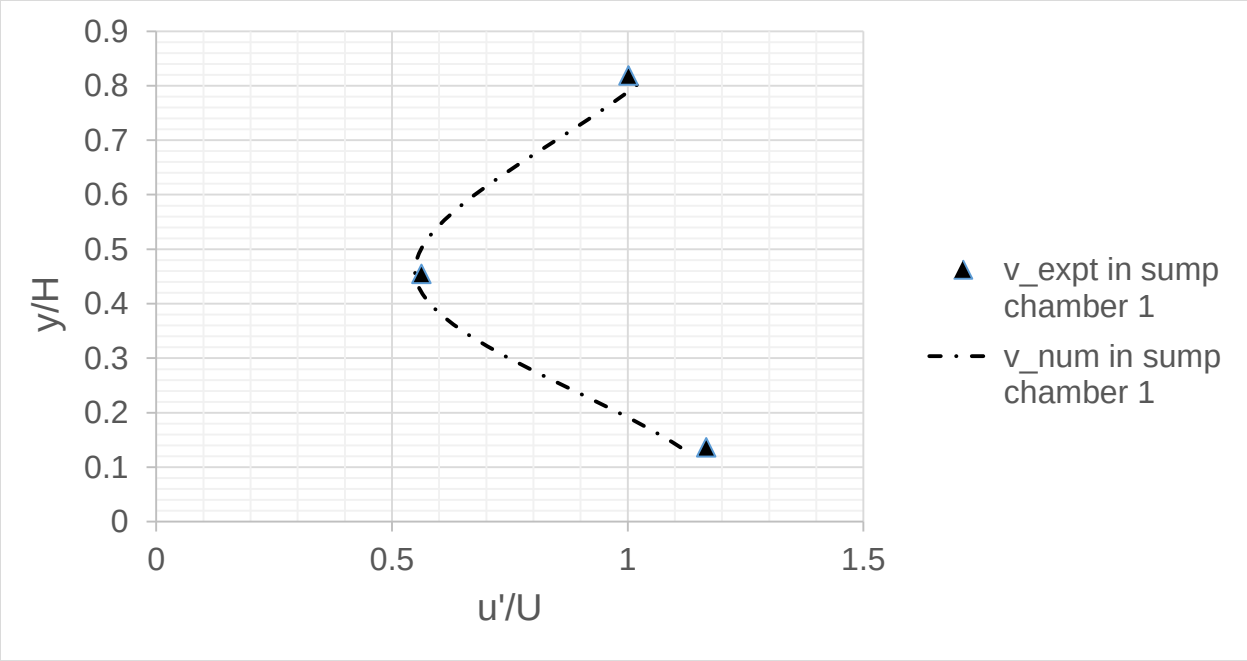

(g)

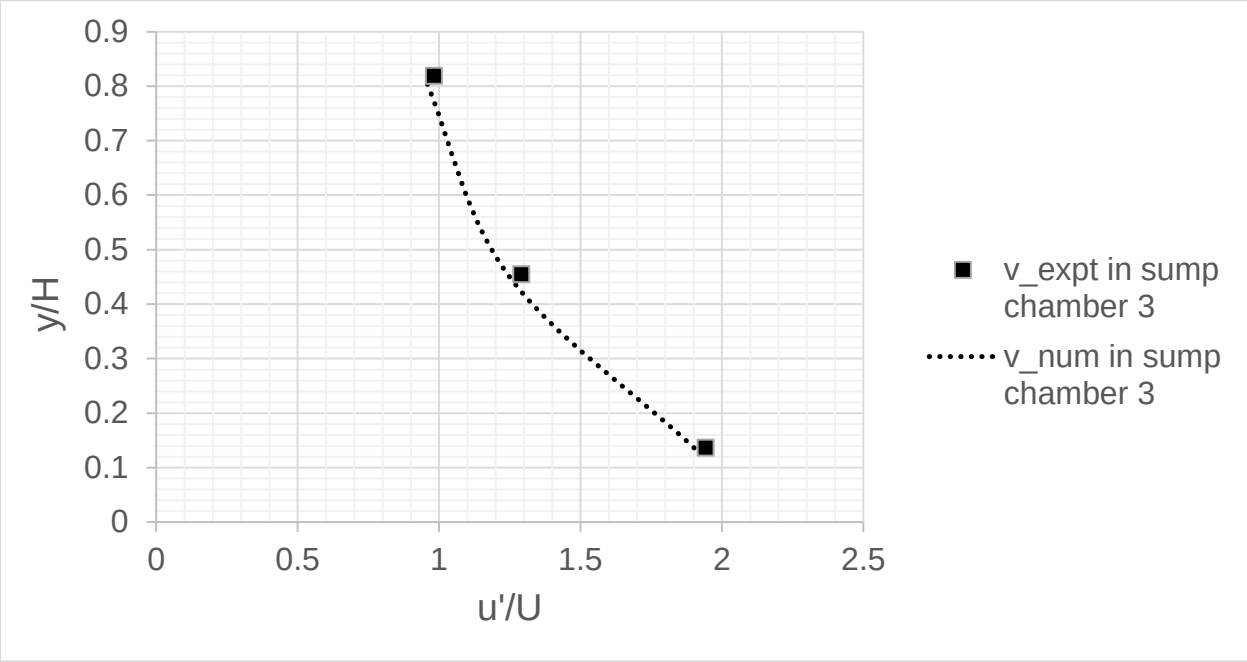

(h)

Figure 6 Non-dimensionalized (a-d) transverse (e-h) axial velocity comparisons at different locations in the sump

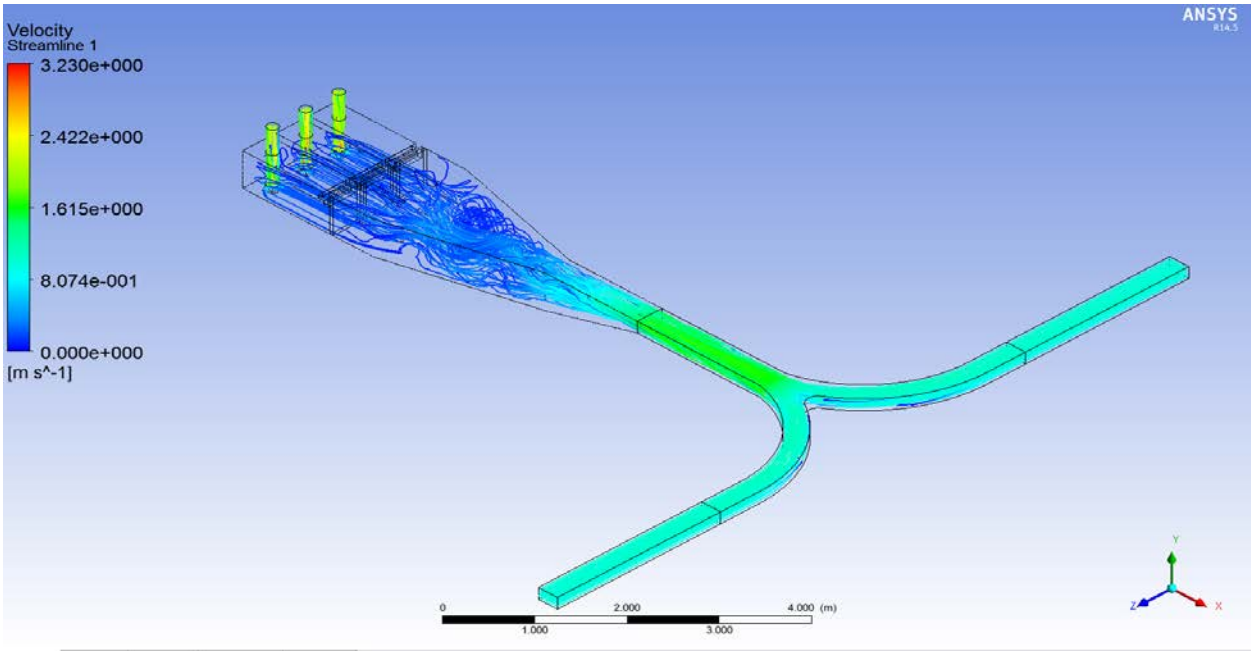

(a)

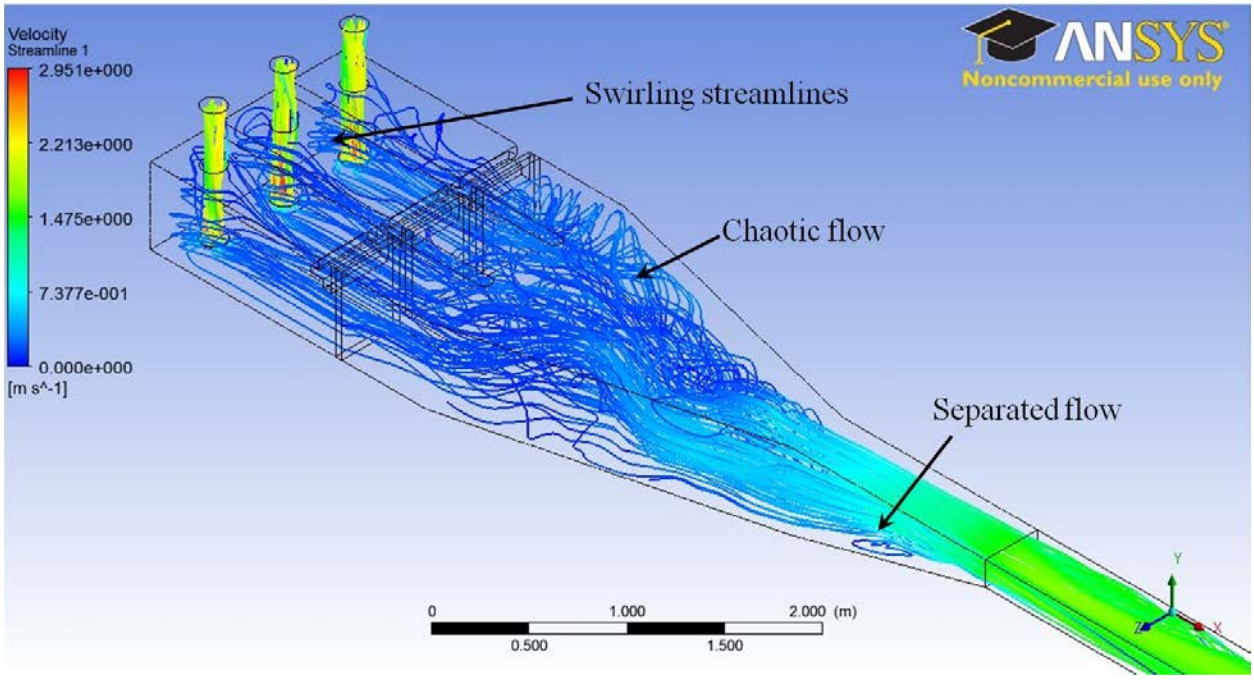

(b)

Figure 7 (a) Full view of the pump sump (b) Magnified view of the transition, forebay and pump bay area.

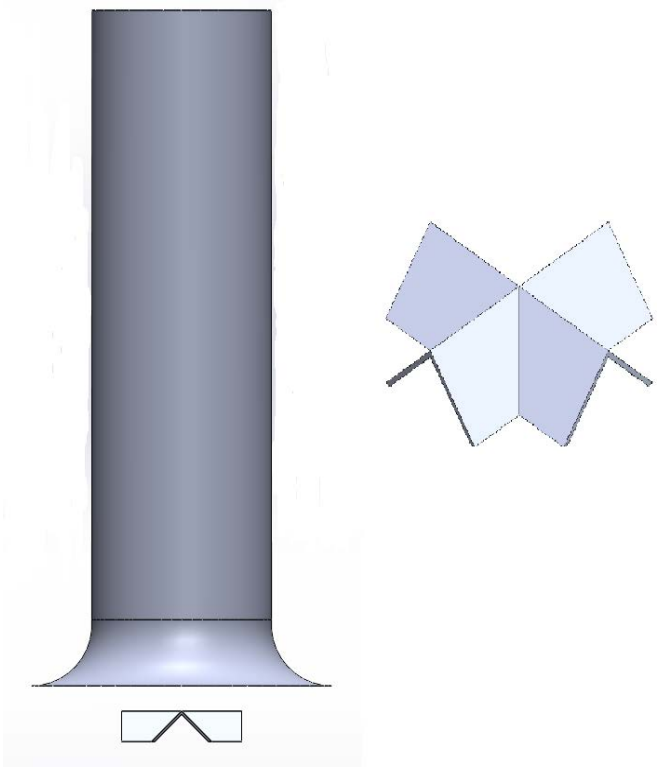

Figure 9 Vortex Breaker used in the present analysis

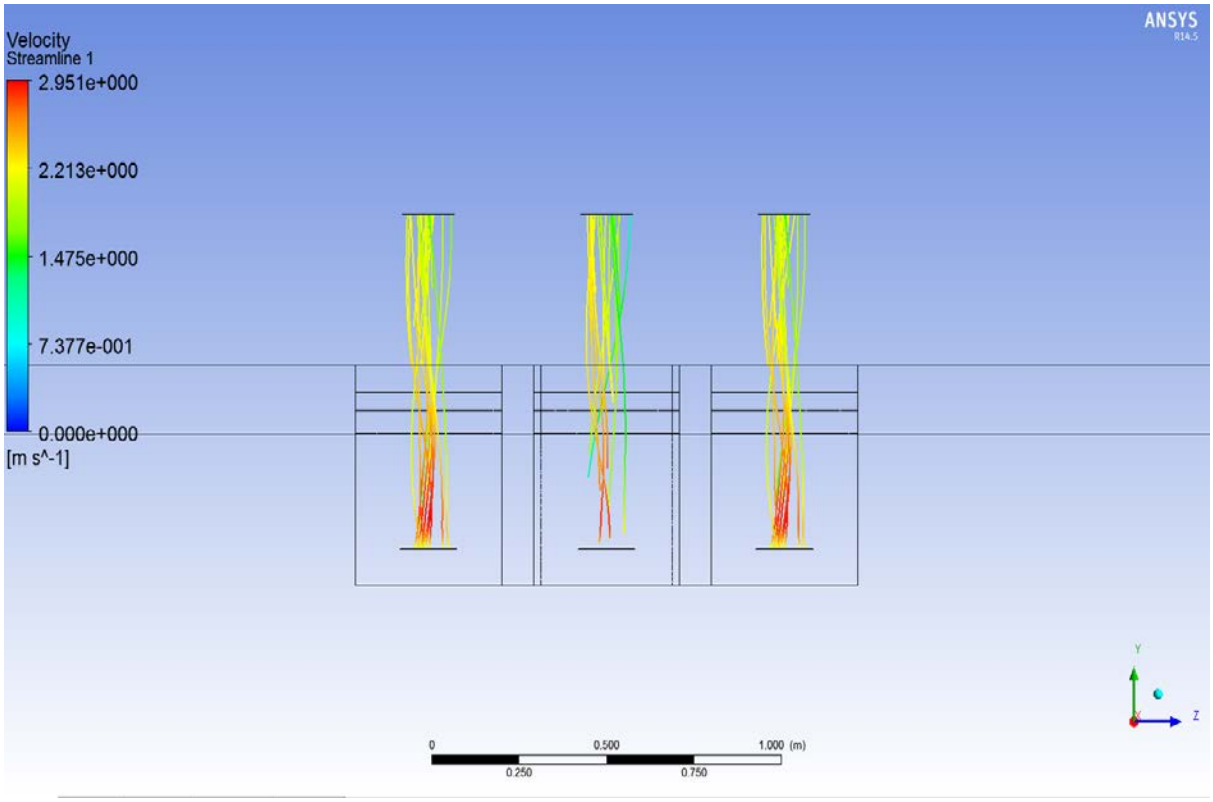
ANSYS
R14.5
Velocity
Streamline 1
2.951e+000
2.213e+000
1.475e+000
7.377e-001
0.000e+000
[m s^-1]
0
0.500
1.000 (m)
0.250
0.750
Y
Z

(a)

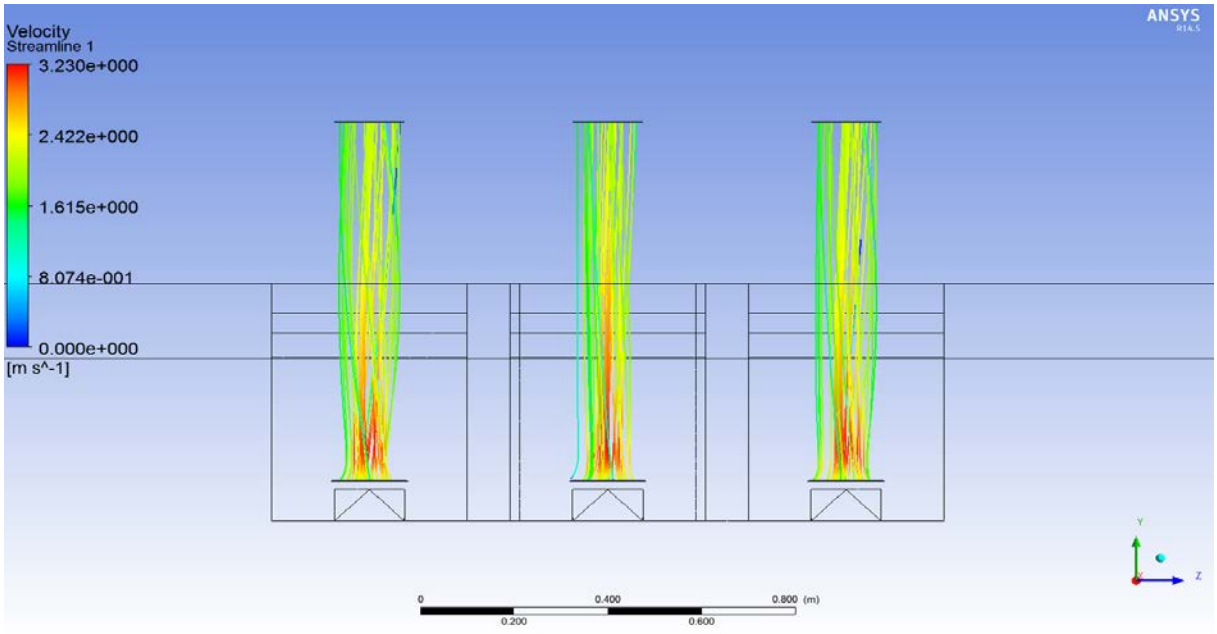
ANSYS
R14.5
Velocity
Streamline 1
3.230e+000
2.422e+000
1.615e+000
8.074e-001
0.000e+000
[m s^-1]
0
0.400
0.800 (m)
0.200
0.600
Y
Z

(b)

Figure 10 Stream lines (a) without (b) with vortex suppression device

Table 1. Solution methods

Terms	**Spatial Discretization method**
Pressure	Standard
Momentum	Second Order Upwind
Turbulent Kinetic Energy	First Order Upwind
Turbulent Dissipation Rate	First Order Upwind

Table 2. Section for velocity measurements

Plane of calculation	**Position**	**Approximate location**
[1]	Start of transition region	24.75 D away from backwall of pump bay
[2]	Start of forebay region	18 D away from backwall of pump bay
[3]	Middle of forebay	13.25 D away from backwall of pump bay
[4]	Central section of Pump bay	4 D away from backwall of pump bay

Table 3 Swirl angles computed experimentally and numerically without vortex suppression devices

Case No.	**Pump 1**		**Pump 2**		**Pump 3**	
	Numerical	Expt.	Numerical	Expt.	Numerical	Expt.
1	3.92°	3.40°	2.54°	2.34°	2.31°	2.16°
2	X	X	2.73°	2.52°	3.81	3.66°
3	4.36°	4.12°	X	X	X	X

Table 4 Swirl angles computed experimentally and numerically with vortex suppression devices

Case No.	**Pump 1**		**Pump 2**		**Pump 3**	
	Numerical	Expt.	Numerical	Expt.	Numerical	Expt.
1	1.10°	0.91°	0.96°	0.91°	0.51°	0.68°
2	X	X	0.74°	0.91°	1.01^{o}	0.68°
3	0.91°	1.14°	X	X	X	X

References

[1] Melville, B. W., Ettema, R., and Nakato, T. (1993). Flow Problems at Water Intake Pump Sumps–A Review. EPRI Research Project RP3456-01 Final Report, IIHR, The University of Iowa, Iowa City, IA, USA.

[2] Hydraulic Institute, Pump Intake Design, ANSI/HI 9.8-1998, (1998).

[3] Tullis, J. P. (1979). Modeling in design of pumping pits. Journal of the Hydraulics Division, 105(9), 1053-1063.

[4] Sweeney, E., and Elder, R. A. (1982). Pump sump design experience: summary.Journal of the Hydraulics Division, 108(HY3), 361-77.

[5] Knauss J (ed) (1987) Swirling flow problems at intakes. IAHR hydraulic structures design manual. A.A. Balkema, Rotterdam.

[6] Daggett, L. L., and Keulegan, G. H. (1974). Similitude Conditions in Free-Surface Vortex Formations (No. AEWES-Misc-Paper-H-74-1). Army Engineer Water Ways Experimental Station Vicksburg Miss.

[7] Hecker, G. E. (1981). Model-Prototype Comparison of Free Surface Vortices. Journal of the Hydraulics Division, 107(10), 1243-1259.

[8] Tagomori, M., & Gotoch, M. (1989). Flow patterns and vortices in pump-sumps. In Proceedings of the International Symposium on Large Hydraulic Machinery, China Press, Beijing, China, May (pp. 28-31).

[9] Takata, T., Kawata, Y., Kobayashi, T., Taniguchi, N., and Morinishi, Y. (1992, December). Large eddy simulation of unsteady turbulent swirl flow in a pump intake. In Computational Fluid Dynamics' 92 (Vol. 1, pp. 255-261)

[10] Lin-guang, L. U. (2000). Basic flow patterns and optimum hydraulic design of a suction box of pumping station, Journal of Hydrodynamics, Ser. B, 12(4), 46-51

[11] Constantinescu, G. S., and Patel, V. C. (1998). Numerical model for simulation of pump-intake flow and vortices. Journal of Hydraulic Engineering, 124(2), 123-134

[12] Chuang, W. L., and Hsiao, S. C. (2011). Three-dimensional numerical simulation of intake model with cross flow. Journal of Hydrodynamics, Ser. B, 23(3), 314-324.

[13] Chen H. X., and Guo, J. H. (2007). Numerical simulation of 3-D turbulent flow in the multi-intakes sump of the pump station. Journal of Hydrodynamics, Ser. B, 19(1), 42-47.

[14] Desmukh, T. S., and Gahlot, V. K. (2011). Numerical study of flow behavior in a multiple intake pump sump. International Journal of Advanced Engineering Technology, 2, 118-128.

[15] Launder, B. E., and Spalding, D. B. (1974). The numerical computation of turbulent flows. Computer methods in applied mechanics and engineering, 3(2), 269-289.

[16] Li, S., Lai, Y., Weber, L., Silva, J. M., and Patel, V. C. (2004). Validation of a three-dimensional numerical model for water-pump intakes. Journal of Hydraulic Research, 42(3), 282-292.

[17] Patankar, S. (1980). Numerical heat transfer and fluid flow. CRC Press.